Journal of Petroleum Science and Engineering 109 (2013) 26–37

Contents lists available at ScienceDirect

Journal of Petroleum Science and Engineering

journal homepage: www.elsevier.com/locate/petrol

Fines-migration-assisted improved gas recovery during gas field depletion

Thi K. Phuong Nguyen, Abbas Zeinijahromi, Pavel Bedrikovetsky *

Australian School of Petroleum, The University of Adelaide, Adelaide, 5000 SA, Australia

ARTICLE INFO

Article history:
Received 2 September 2011
Accepted 1 August 2013
Available online 9 August 2013

Keywords:
Fines migration
Gas reservoir
Water production
Gas recovery
Formation damage

ABSTRACT

The core permeability decline during corefloods with varying water composition, especially with low salinity water, has been widely reported in the literature. It has often been explained by the lifting, migration and subsequent plugging of pore throats by fine particles, which has been observed in numerous core flood tests with altered water composition. In this work, the concept of using this permeability decline in order to decrease water production during pressure depletion in gas field is investigated. The small volume injection of fresh water into an abandoned watered-up well in order to slow down the encroaching aquifer water is discussed. Equations for two-phase immiscible compressible flow with fines migration and capture have been derived. In large scale approximation, the equations are transformed to the black-oil polymer flooding model. The performed reservoir simulation shows that injection of fresh water bank significantly decreases water production and improves gas recovery.

1. Introduction

The invasion of aquifer water into a gas reservoir during pressure depletion development results in watering-up the production wells, in by-passing the gas by the encroaching water and in the increased amounts of the residual gas trapped behind the water front. Usually, gas wells are abandoned after reaching 20–30% water cut with a decreased well life time. Depending on the reservoir heterogeneity, the residual gas saturation may reach 50–60% with low gas recovery factor (Braedley, 1987). Slowing down the encroached water helps to increase gas recovery during pressure depletion in gas fields. In gas field planning and developments, the water speed may be decreased by reduction in the production rates; management of the total gas production by redistribution of rates in order to reduce rates in the wells near to gas–water contact. Injection of barrier fluids into swept zones is another solution to the water production problem during gas field exploitation (Karp et al., 1962; Zaitoun and Pichery, 2001).

Permeability decline due to fines migration has been widely reported in the literature. Usually, it is explained by the mobilization of fine particles, their migration and plugging of small pores by size exclusion capture (Muecke, 1979; Tiab and Donaldson, 2004), see Figs. 1 and 2. The fine particle equilibrium on the grain surface, pore wall or in the clay booklet is determined by drag, lifting, adhesion, electrostatic and gravitational forces (Sharma and Yortsos, 1987c; Schechter, 1992; Jiao and Sharma, 1994; Khilar and Fogler, 1998; Bergendahl and Grasso, 2000; Freitas and Sharma, 2001; Schembre and Kovscek, 2004; Takahashi and Kovscek, 2010). The fine particle release by the increase in flow velocity has been investigated in several laboratory studies (Miranda and Underdown, 1993; Ochi and Vernoux, 1998). The mobilization of fines due to water composition alteration has also been widely addressed (Lever and Dawe, 1984; Valdya and Fogler, 1992; Khilar and Fogler, 1998). The release of the retained fines by changing water–oil saturations and their detachment by the capillary force acting on the water–oil menisci have been recently observed during core flood studies with low salinity water (Kumar et al., 2010; Fogden, et al., 2011; Mahani et al., 2012).

In the present paper, fines mobilization with the consequent permeability decline is considered as a possible mechanism of decreasing the encroaching water velocity (Fig. 3). Injection of a small volume of fresh water into an abandoned watered-up well may cause fines mobilization, creating a low permeable barrier against the invading water. Invasion of aquifer water with the composition different from the formation water, slowing it down due to reservoir fines release and the consequent permeability decline in the swept zone, is also discussed as a natural mechanism of the water production reduction. The estimation of the effects of induced and natural fines migration of gas recovery is based on the mathematical modeling.

The classical advective–diffusive attachment–detachment filtration model assumes simultaneous first-order kinetics for the particle capture and detachment (Civan, 2007; Ju et al., 2007; Bradford and Torkzaban, 2008; Lin et al., 2009; Bradford et al., 2009; Civan, 2010; Gitis et al., 2010; Massoudieh and Ginn, 2010;

* Corresponding author. Tel.: +61 8 8303 4345; fax: +61 8 830 3 3082.
E-mail addresses: pavel.russia@gmail.com, pavel@asp.adelaide.edu.au (P. Bedrikovetsky).

0920-4105/$ - see front matter © 2013 Elsevier B.V. All rights reserved.
http://dx.doi.org/10.1016/j.petrol.2013.08.020

Nomenclature

c_a	polymer adsorption isotherm
c^0	initial concentration of suspended particles
c_v	variance coefficient
f	fractional flow of water
F_{ad}	adhesion force, $M\,L\,T^{-2}$, N
F_d	drag force, $M\,L\,T^{-2}$, N
F_e	electrostatic force, $M\,L\,T^{-2}$, N
F_g	gravitational force, $M\,L\,T^{-2}$, N
F_l	lifting force, $M\,L\,T^{-2}$, N
k	absolute permeability, L^2, mD
k_0	initial absolute permeability, L^2, mD
k_{rg}	gas relative permeability
k_{ro}	oil relative permeability
k_{rw}	water relative permeability
L	reservoir size, L, m
l_d	lever for drag force, L, m
l_n	lever for normal force, L, m
p	pressure, $M\,L^{-1}\,T^{-2}$, Pa
R	gas constant, J/mol^{-1} θ^{-1}, J/mol K
s	water saturation
t	time, T, s
T	absolute temperature, θ, K
t_D	dimensionless time, PVI
$\vec{U}$	flow velocity, $L\,T^{-1}$, m/s
z	compressibility coefficient

Greek letters

γ	brine ionic strength, mol L^{-3}, mol/m^3
ϕ	porosity
μ_o	oil dynamic viscosity, $M\,L^{-1}\,T^{-1}$, CP
μ_w	water dynamic viscosity, $M\,L^{-1}\,T^{-1}$, CP
β	formation damage coefficient
ε	torque ratio
λ_s	filtration coefficient for straining, L^{-1}, 1/m
ρ_a	gas density at standard condition, $M\,L^{-3}$, kg/m^3
ρ_g	gas density, $M\,L^{-3}$, kg/m^3
ρ_s	rock density, $M\,L^{-3}$, kg/m^3
ρ_w	water density, $M\,L^{-3}$, kg/m^3
σ	volumetric concentration of captured particles, L^{-3}, 1/m^3
σ_a	volumetric concentration of attached particles, L^{-3}, 1/m^3
σ_{ao}	initial volumetric concentration of attached particles, L^{-3}, 1/m^3
σ_{cr}	critical volumetric concentration of strained particles, L^{-3}, 1/m^3
σ_s	volumetric concentration of strained particles, L^{-3}, 1/m^3

Abbreviations

RRF	maximum resistance factor

Gravelle et al., 2011). The detachment rate is assumed to be proportional to the difference between the current and critical parameters like velocity, concentrations, etc. The detailed theory for dependency of the capture kinetics (filtration) coefficient on the pore scale parameters for particle attachment was developed (Nabzar et al., 1996; Chauveteau et al., 1998; Rousseau et al., 2008), while the detachment kinetics coefficients are the empirical constants usually determined by their tuning with the break-through concentration (Ju et al., 2007; Tufenkji, 2007; Civan, 2010). Another shortcoming of the classical filtration model with the kinetics of particle detachment is the asymptotical stabilization of the retention concentration and permeability when time tends to infinity, while the fines release due to an abrupt pressure gradient increase or under salinity alternation happens almost instantly (Miranda and Underdown, 1993; Khilar and Fogler, 1998). Corefloods with the sharp rate increase show an immediate abrupt permeability response (Lever and Dawe, 1984; Ochi and Vernoux, 1998) while the quasi linear classical filtration model predicts a smooth asymptotic response with time delay. A particle detachment is governed by the mechanical equilibrium of the retained particles on the internal filter cake or matrix surface; the mechanical equilibrium is determined by the moment

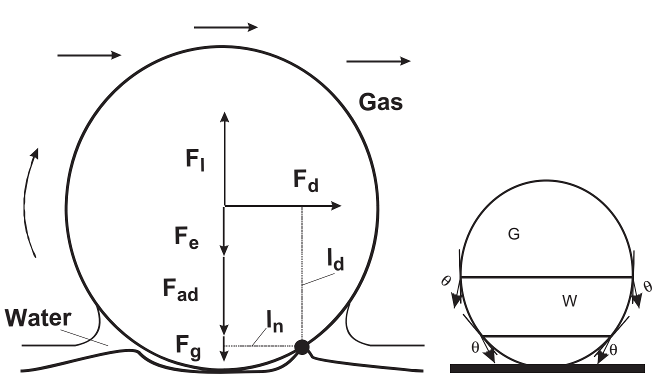

Fig. 1. Forces exerting upon a fine particle in the moving water.

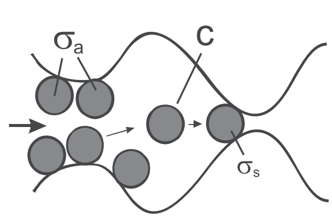

Fig. 2. Schema of pore plugging by the mobilized particles.

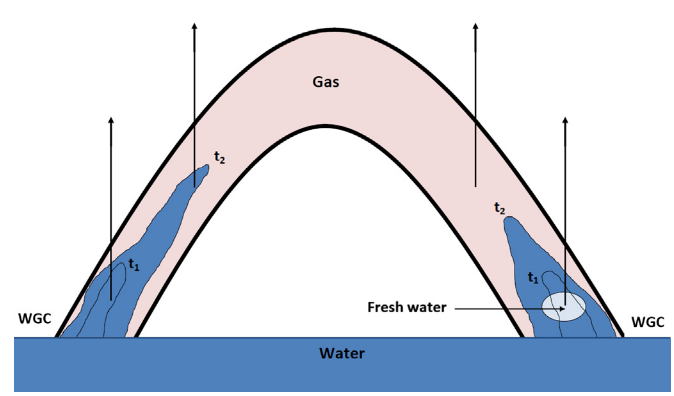

Fig. 3. Schematic for enhanced gas recovery assisted by fines migration in the anticlinal gas reservoir by fresh water injection.

balance of electrostatic, drag, lifting and gravity forces, acting on a single particle sitting on a grain or on the internal cake surface (Freitas and Sharma, 2001; Civan, 2007; Takahashi and Kovscek, 2010). Yet, the advective–diffusion equation with the kinetic detachment term does not reflect the mechanical equilibrium of the particle; the detachment term is not affected by the forces exerting on a single particle. Recently developed deep bed filtration model with the migrating layer of the particles, attached in the secondary energy minimum (Yuan and Shapiro, 2010b) also does not accounting for forces exerted on the retained particles.

Since the forces depend on the particle and pore sizes, which are stochastically distributed in natural rocks, the detailed modeling studies on micro (pore) scale have been carried out (Payatakes et al., 1973, 1974). These includes population balance models (Sharma and Yortsos, 1987; Bedrikovetsky, 2008), random walk equations (Cortis et al., 2006; Shapiro, 2007; Lin et al., 2009; Yuan and Shapiro, 2010a) and direct pore scale simulation (Bradford et al., 2009). The population balance and random walk models, as well as the large scale phenomenological models, use non-equilibrium detachment rate equations with empirical kinetics coefficients and do not reflect forces, exerting on a single particle.

The modified particle detachment model uses the maximum (critical) retention function instead of the kinetics expression describing the detachment rate. If the retention concentration does not exceed its maximum value, particle capture occurs according to the classical model of deep bed filtration; otherwise, the maximum retention concentration value, which depends on flow velocity and water composition, holds (Bedrikovetsky et al., 2011). The maximum retention concentration is determined by the condition of mechanical equilibrium of the particle on the matrix or internal cake surface, which is described by the torque balance of electrostatic, drag, lifting and gravitational forces. The analytical solution for the continuous suspension injection with permeability decrease until reaching the maximum retained concentration was successfully matched with the core flooding data. The modified particle detachment model was validated by comparison with numerous laboratory studies (Zeinijahromi et al., 2011, 2012). Yet, the model was developed for single phase flows only.

In the present paper, basic equations for two-phase immiscible compressible flow with fines mobilization and capture are derived. In this model, the particle detachment is governed by the maximum retention function, which depends on water composition, velocity and water saturation. Large scale approximation of the system corresponds to an instant capture of the released fines. Neglecting the saturation dependency of the maximum retention function allows converging the proposed governing equations into the black-oil model for polymer injection. The reservoir simulation as performed using Eclipse-100 allows the estimation of gas recovery after injection of fresh water bank into abandoned watered-up gas wells.

The structure of the paper is as follows. Firstly, we describe the reservoir physics of fines mobilization and the consequent creation of a low permeability barrier against the invading aquifer water. Then, the derivation of the governing equations for gas–water flow with fine particles follows (Section 3). Asymptotical large scale approximation of the basic system is presented in Section 4. Section 5 contains the transformation of the mathematical model for 2-phase flow with fines into the polymer injection model. The results of the reservoir simulation are discussed in Section 6.

2. Physics mechanisms of fines migration assisted incremental gas recovery

Mobilization of fines due to changes in formation water (decreased salinity, increased pH, and higher temperature), their migration and straining in small pores with consequent permeability decline have been observed in numerous field applications (Bennion et al., 1996, 2000; Bennion and Thomas, 2005, Byrne and Waggoner, 2009, Byrne et al., 2010). Let us explore the possibility of using fresh water as a barrier fluid to decrease water invasion into gas reservoir with the strong water support pressure blow down. The essence of the proposed method is the creation of a low permeable barrier against the invasion of the aquifer water into the gas field during its depletion. The barrier is created by injection of fresh water into an abandoned watered-up well.

Fig. 1a shows the forces acting on a fine particle located on the grain surface or on the internal cake: drag, lift, electric, adhesion and gravitational forces. The picture corresponds to the initial connate water saturation in a gas field before the invasion of aquifer water. Usually a well is abandoned when water cut reaches the value $f=0.25$–0.35, which corresponds to water saturation in the range of 0.4–0.8 depending on the relative permeability of the gas and water phases. Water saturation increases during the fresh water bank injection. Since water viscosity highly exceeds gas viscosity, drag and lifting forces exerting upon the fine particle in gas phase are negligibly smaller than those in water. Therefore, drag and lifting forces exerting upon the fine particle increase during the increase with increasing water saturation. It is assumed that the formation rock is water-wet in gas reservoir; hence, a water film covers the rock surface. The electrostatic force exerting on the tangent point of the particle, which is immersed in the water film, remains constant during water saturation increase. The length of the contact curve between gas, water and particle interfaces increases where the water film thickness rises from the initial level up to the center of the particle's sphere (Fig. 1b). Consequently, the corresponding adhesion force, equal to the product of the length of the curve and the gas–water interfacial tension, also increases. Further increase of water level results in decrease in the adhesion force which tends to zero when the water layer completely covers the particles. The gravitational force, which in reality is the buoyancy force, decreases with increase of water saturation since the water density is much higher than that of gas. The main attaching force alternation during the sweet water injection is the decrease of salinity resulting in decrease of electrostatic force, attaching fines to the grain surface. The above physics schema for fines release during two-phase flow has been developed by Muecke and experimentally verified by Sarkar and Sharma (1990).

The mobilized fines migrate in the porous space until they meet the smaller pores, which they strain. Fig. 2 shows the detachment of fine particles after arrival of the fresh water front, its flow inside the pore and size exclusion of migrated particles in thin pore throats resulting in the permeability decline. Here the strained particle is shown to be larger than the pore. Yet, the particles do not need to be larger than pore throat size to block the flow path: according to the 1/3–1/7 rule, all particles larger than 1/3rd of the mean pore radius are strained by bridging or plugging (Van Oort et al., 1993; Khilar and Fogler, 1998).

The above mechanisms of fines mobilization due to water salinity decrease with consequent capture and permeability reduction can be applied for a creation of a low permeability barrier against the invaded water. Fig. 3 shows propagation of water from the aquifer towards production wells during gas field depletion. Minimum pressures during production from wells 1 and 2 have been reached near to their wellbores, so the pressure gradients from the aquifer cross the location points for wells 1 and 2 on the map. Therefore, the central lines of the water fingers from the aquifer also cross the location points for wells 1 and 2. Fig. 3 shows the position of gas–water contact when the wells 1 and 2 are already watered-out. Pressure builds up near the producers 1 and 2 after their abandonment. Minimum pressures over the area are reached near the producing wells 3–7. Therefore, the invaded water moves towards producers 3–7. Injection of small portions of fresh water into wells 1 and 2 after their abandonment causes fines release and slowing down the water fingers. The consequent permeability reduction prolongs dry production period of gas and decreases water production.

Fig. 3 schematically shows the invasion of aquifer water into a gas reservoir, flooding the down-dip producer, further propagation of the water finger towards the up-dip producer and subsequent abandonment (left hand side of the figure). The right hand side of Fig. 3 shows the water finger propagation through the point of the minimum reservoir pressure, which is in the production well vicinity. The gray spot around the abandoned producer corresponds to injected fresh water and the consequent reduced permeability. The low permeable barrier is located at the center of the invaded water tongue, slowing down the invaded water and resulting in the prolongation of the exploitation period of the up-dip well. Consequently, this results in the increased gas recovery before the abandonment of the second well.

3. Mathematical model for gas–water flow with fines migration

The modified particle detachment model uses the maximum (critical) retention function to describe the fine particles detachment (Bedrikovetsky et al., 2011). In this model, the particle capture continues according to the classical deep bed filtration theory until the concentration of retained particles reaches its maximum, determined by the static equilibrium of force torques acting on a particle. Changes in fluid velocity or composition may abruptly reduce the maximum retained concentration below its current value, leading to the instantaneous particle release. To simplify the model, all particles are assumed to be spheres of equal radii made of the same material. Pores are represented by cylindrical tubes and are assumed to be filled with gas. These assumptions are significant and require that the model be matched to laboratory data prior to its use. However, once it is matched to a specific set of data, the effect of changes to velocity or water composition can be investigated without the need for additional laboratory data.

The main forces considered to act on a particle on the surface of a pore or internal particle cake are drag, lift, gravitational, adhesion and a total electrostatic force (Fig. 1). Drag and lift are caused by the gas flow over a particle and act so to detach the particle from the pore wall. Both forces increase with increasing flow velocity, particle radius and the fluid viscosity. The adhesion force acting on the wetting contour in the contact "water–gas–particle" points attach the particle to the grain surface. The gravitational force is the buoyant weight of the particle. The total electrostatic force describes the interaction of a particle and pore wall at very small separations and is independent of fluid velocity. For the purposes of this model, the total electrostatic force is taken as the maximum value of the sum of the van der Waals, electrical double layer and Born forces as described by Derjaguin, Landau, Verwey and Overbeek (DLVO) theory (see Derjaguin (1989) and Khilar and Fogler (1998) for explicit formulae of the electrostatic force). The van der Waals force depends primarily on the Hamaker constant, which is determined by the particle and rock mineralogical compositions; this force is largely independent of changes in water composition (Israelachvili, 1992). However, the electrical double layer force does depend on water composition, specifically on the ionic strength and pH. Hence, it is via the electrical double layer force that changes to salinity and pH affect the force balance and maximum retention concentration. Born's force also depends on the fines and grains mineralogy via the Hamaker constant. Typically, for clastic reservoir rocks, the total attractive electrostatic force decreases as the water salinity decreases and pH increases. A limitation of this modeling approach is that, to be accurate, it must consider all significant forces acting on a particle. The above forces are considered to be the most significant although other forces exist, such as non-DLVO surface forces (Israelachvili, 1992; Khilar and Fogler, 1998; Takahashi and Kovscek, 2010).

The static equilibrium of a particle is determined by the balance of torques from the main forces. The dimensionless erosion number is introduced as the ratio between the detaching and attaching torques:

$$\varepsilon = \frac{F_d l_d + F_l l_n}{(F_e + F_{ad} + F_g) l_n} \tag{1}$$

where F_d, F_l, F_e, F_{ad} and F_g are the drag, lifting, electrostatic, adhesive and gravitational forces, respectively (see Bedrikovetsky et al. (2011), for explicit formulae for the above forces); l_d and l_n are the corresponding levers for the drag and normal forces (Fig. 1). A particle is released if the erosion number exceeds unity. This may occur due to an increase in the drag and lift forces (because of an increase in flow velocity) or a decrease in the electrostatic force (because of a decrease in the water salinity or other change in water composition). The maximum concentration of retained particles is a function of the erosion number and of water saturation for any porous media (Bedrikovetsky et al., 2011). The derivation of equation

$$\sigma = \sigma_{cr}(\varepsilon) \tag{2}$$

for an average cylindrical capillary of the porous medium is based on the torque force equilibrium. Fig. 4 shows the results of matching the theoretical model (Eq. (2)) to the laboratory data on the sequential core flood by water with the decreasing salinity (Lever and Dawe, 1984).

Fig. 1 shows that the adhesion force depends on the radius of the boundary curve between the gas, solid and wetting water interfaces, which depends on the thickness of the water layer, i.e. of saturation. The saturation value also determines the fraction of

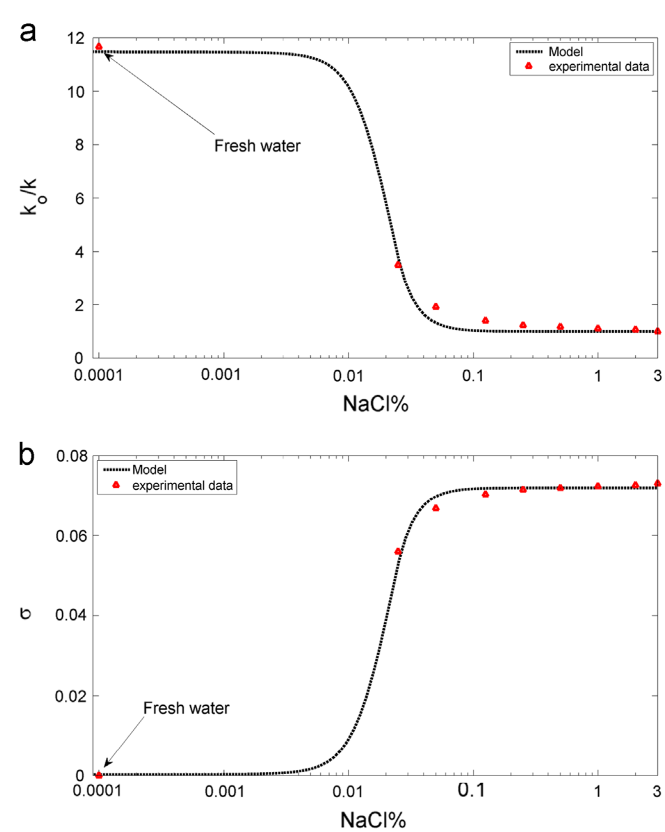

Fig. 4. Maximum saturation function as calculated from laboratory tests by Lever and Dawe (1984) and by theoretical model: (a) normalized reciprocal to permeability, (b) maximum retained fines concentration versus water salinity.

the matrix surface wetted by water, where the attached fines are exerted upon by the pressure gradient in water and the gas–matrix surface (Fig. 1). Therefore, the maximum retention concentration is also a function of saturation

$$\sigma = \sigma_{cr}\,(\varepsilon, s) \tag{3}$$

Following Pang and Sharma (1997) and Mojarad and Settari (2007), it is assumed that the inverse to normalized permeability $k(\sigma)/k_0$ is a linear function of the retained particle concentration:

$$\frac{k_0}{k(\sigma)} = 1 + \beta\sigma \tag{4}$$

where β is the so-called formation damage coefficient. If β is high, even a small retained concentration causes a high permeability reduction. The formation damage coefficient for straining is assumed to be much greater than that for attachment, i.e. the detachment of fines causes a negligibly small permeability increase while the plugging of pore throat results in a significant decrease of permeability (Fig. 2). So, σ in Eq. (4) corresponds to the concentration of strained particles.

Let us discuss a system of two-phase flow in porous media with varying water salinity that lifts the fine particles. For simplicity, we assume that the volumetric concentrations of attached and retained particles are negligibly small if compared to the porous space, i.e. the fine particles retention does not affect the rock porosity. We also assume no diffusion and capillary pressure. Reservoir temperature is assumed to be constant. Accounting for temperature variation due to water influx is achieved by including the energy conservation equation into the governing system. Other assumptions include incompressibility of water, constant water and gas viscosities as given by the equation of state for real gas with the pressure-dependent z-factor.

Mass balance for water under the assumption of water incompressibility is (Cinar et al., 2006, 2007)

$$\phi\frac{\partial s}{\partial t} + \vec{\nabla}\vec{U}_w = 0 \tag{5}$$

where $\vec{U}_w$ is the three dimensional vector for the water flux:

$$\vec{U}_w = (u_{xw}, u_{yw}, u_{zw})$$

The pressure difference between water and gas phases is equal to capillary pressure

$$p_g - p_w = \frac{\sigma\cos\theta}{\sqrt{k/\phi}}J_c(s) \tag{6}$$

The equation for mass balance of gas phase is

$$\phi\frac{\partial}{\partial t}\left(\frac{p_g}{z(p_g)}(1-s)\right) + \vec{\nabla}\left\{\frac{p_g}{z(p_g)}\vec{U}_g\right\} = 0 \tag{7}$$

where the density of real gas can be determined by

$$\rho_g = \frac{p\rho_a}{z(p)RTp_a} \tag{8}$$

Here, $z(p_g)$ is the compressibility coefficient.

The mass balance of suspended, attached and strained particles is

$$\frac{\partial}{\partial t}\left[\phi sc\rho_w + (\sigma_a + \sigma_s)\rho_s\right] + \vec{\nabla}(c\rho_w\vec{U}_w) = \vec{\nabla}(Ds\rho_w\vec{\nabla}c) \tag{9}$$

The fines, attached by electrostatic and adhesion forces coat the grains and form the lining covers while the strained particles plug the pore throats (Fig. 2).

Size exclusion capture of mobilized fine particles in small pores is described by the equation of the linear kinetics (Bedrikovetsky, 2008)

$$\rho_s\frac{\partial\sigma_s}{\partial t} = \lambda_s(\sigma_s)c\vec{U}_w\rho_w \tag{10}$$

Here, the straining rate is proportional to water flux $\vec{U}_w$ since the mobilized fine particles are transported by the water phase.

The mass balance of salt in the aqueous phase assumes low salt concentration not affecting the aqueous phase density ρ_w:

$$\frac{\partial}{\partial t}(\phi\gamma) + \vec{\nabla}(\gamma\vec{U}_w) = \vec{\nabla}(Ds\vec{\nabla}\gamma) \tag{11}$$

Water salinity affects the attaching fine-grain electrostatic force, so the erosion ration in (3) is salinity-dependent.

The modified two-phase flow Darcy's law accounting for permeability damage to water is

$$\vec{U}_w = -k\frac{k_{rw}(s)}{\mu_w(1+\beta\sigma_s)}\vec{\nabla}p_w, \tag{12}$$

The modified two-phase flow Darcy's law for gas phase is

$$\vec{U}_g = -k\frac{k_{rg}(s)}{\mu_g}\vec{\nabla}p_g \tag{13}$$

Finally, the governing system for two-phase gas–water flow with fines mobilization due to the decrease of water salinity and consequent reduction of relative permeability for water consists of the following equations: (1) mass balance for compressible gas (7); (2) volumetric balance of incompressible water (5); (3) mass balance of suspended, attached and strained particles (9); size exclusion retention rate (10); (4) advective mass transfer of salt in porous space with retained fines (11); (5) modified Darcy's law accounting for permeability reduction due to fines straining (12); and (6) either attachment retention rate or the maximum attachment function (3).

System of nine Eqs. (3), (5)–(7), (9)–(13) determines nine unknowns: σ_a, s, p_w, p_g, c, γ, σ_s, $\vec{U}_w$ and $\vec{U}_g$.

For large length scale L that is the distance between the injection and production well rows, the governing system becomes significantly simpler. The corresponding transformations are presented in the next section.

4. Large scale approximation

Let us introduce the following dimensionless parameters and variables into the governing system for two-phase gas–water flow with fines mobilization and straining:

$$\begin{aligned}
&x_D = \frac{x}{L}, \quad t_D = \frac{1}{\phi LWH}\int_0^t q(\tau)d\tau, \quad S_a = \frac{\sigma_a}{\sigma_{a0}}, \quad S_s = \frac{\sigma_s}{\sigma_{a0}},\\
&C = \frac{\phi c}{\sigma_{a0}}, \quad U_0 = \frac{q}{WH}, \quad u = \frac{U}{U_0} = \frac{UWH}{q},\\
&P_w = \frac{k_0 p_w}{U_0\mu_w L} = \frac{k_0 p_w WH}{q\mu_w L}, \quad P_g = \frac{k_0 p_g}{U_0\mu_w L} = \frac{k_0 p_g WH}{q\mu_w L},\\
&M = \frac{\mu_w}{\mu_g}, \quad \Lambda = \lambda L
\end{aligned} \tag{14}$$

Here, $q(t)$ is the well injection rate, H is the reservoir thickness, W is the distance between injectors in a row and Λ is the dimensionless filtration coefficient. Mobilization of σ_{a0} attached particles results in suspension concentration

$$c^0 = \frac{\sigma_{a0}}{\phi}$$

After substitution of dimensionless phase pressures from (14), Eq. (6) becomes

$$P_g - P_w = \frac{\sqrt{k\phi}\sigma\cos\theta}{U_0\mu_w L} J_c(s) \tag{15}$$

For large length scale L

$$L \gg \frac{\sqrt{k\phi}\sigma\cos\theta}{U_0\mu_w} \tag{16}$$

the dimensionless coefficient in front of the Leverett function in right hand side (15) is significantly smaller than one and capillary pressure can be neglected if compared with phase pressures. From now on the phase pressures are equal p.

Introduce the total flux by adding (12) and (13):

$$\vec{U} = -k\left[\frac{k_{rw}(s)}{\mu_w(1+\beta\sigma_s)} + \frac{k_{rg}(s)}{\mu_g}\right]\vec{\nabla} p \tag{17}$$

The fractional flow for water $f(s,\sigma_s)$ that is the ratio between the water and overall fluxes is calculated from (12) and (17)

$$f(s,\sigma_s) = \left[1 + \frac{k_{rg}(s)\mu_w(1+\beta\sigma_s)}{k_{rw}(s)\mu_g}\right]^{-1} \tag{18}$$

Substitution of dimensionless variables (14) and (18) into mass balance Eqs. (5) and (7) yields

$$\frac{\partial s}{\partial t_D} + \nabla[f(s,S_s)u] = 0 \tag{19}$$

$$\frac{\partial}{\partial t_D}\left(\frac{P(1-s)}{z(P)}\right) + \vec{\nabla}\left\{\frac{P}{z(P)}[1-f(s,S_s)]\vec{u}\right\} = 0 \tag{20}$$

Now let us derive the asymptotical form of the fines migration Eqs. (9)–(11) for large reservoir scale, where the free run length of the particle is negligible at the reservoir length scale. The free run length is reciprocal to filtration coefficient (see Tufenkji, 2007 or Bedrikovetsky, 2008), so the large scale condition is

$$\frac{1}{\lambda_s} \ll L$$

i.e. the dimensionless filtration coefficient for straining

$$\lambda_s L \gg 1 \tag{21}$$

Tending $\lambda_s L$ to infinity in the left hand side of the dimensionalised Eq. (10) under the assumption of limited retention rate results in dimensionless suspended concentration tending to zero, i.e. $c \ll \sigma_{a0}/\phi$. Ignoring the suspended concentration in third Eq. (9) leads to

$$\frac{\partial}{\partial t}(\sigma_a + \sigma_s) = 0$$

i.e.

$$\sigma_s = \sigma_{a0} - \sigma_{cr}(\varepsilon, s) \tag{22}$$

Eq. (22) means that in large scale approximation, where the free particle run length is negligible if compared with the inter-well distance, the lifted fines are immediately captured by size exclusion in porous media. The amount of the strained fine particles becomes equal to the amount of mobilized fines.

In dimensionless form, Eq. (22) becomes

$$S_s = 1 - S_{cr}(\varepsilon, s) \tag{23}$$

Accounting for (23), a governing system of Eqs. (19) and (20) is transformed to the dimensionless equations of volume balance for water

$$\frac{\partial s}{\partial t_D} + \vec{\nabla}\left[f(s, S_{cr}(\varepsilon(\gamma), s))\vec{u}\right] = 0 \tag{24}$$

where

$$f(s, S_{cr}(\varepsilon(\gamma), s)) = \left[1 + \frac{k_{ro}(s)M(1+\beta\sigma_{a0}(1-S_{cr}(\varepsilon,s)))}{k_{rw}(s)}\right]^{-1}$$
$$S_a = S_{cr}(\varepsilon, s), \quad \varepsilon = \varepsilon(\gamma, (Uf/\phi s), s) \tag{25}$$

for gas mass balance

$$\frac{\partial P(1-s)}{\partial t_D} + \vec{\nabla}\left\{P[1-f(s,S_s)]\vec{u}\right\} = 0 \tag{26}$$

and the modified Darcy's law for two-phase flow and permeability damage in pores where water moves is

$$\vec{u} = -\left[\frac{k_{rw}(s)}{1+\beta\sigma_{a0}(1-S_{cr}(\varepsilon(\gamma),s))} + k_{rg}(s)M\right]\vec{\nabla} P \tag{27}$$

Substitution of dimensionless variables (14) into the equation for mass balance of salt (11) results in the appearance of Schmist's number DWH/qL in right hand side of Eq. (11). Therefore, for large scale where

$$L \gg \frac{DWH}{q} \tag{28}$$

the dispersion / diffusion flux is negligible if compared with the advective flux. Eq. (11) becomes

$$\frac{\partial(\gamma s)}{\partial t_D} + \vec{\nabla}(\gamma f \vec{u}) = 0 \tag{29}$$

System of Eqs. (24), (26)–(27), (29) describes the injection of low salinity water into gas reservoir with water support and further gas–water flow with fines lifting, migration, capture and subsequent permeability damage at the reservoir length scale. Number of unknowns in large scale approximation is reduced to four: saturation s, dimensionless pressure P, salt concentration γ and dimensionless total velocity u. The minimum length L where the large scale approximation applies is determined by maximum of estimates (16), (21) and (28).

The core scale flows are described by the full system of governing Eqs. (3), (5)–(7), (9)–(13). The coreflood data must be treated using the full system.

In the next section we transform the model for water–gas flow with fines migration into the system of equations for polymer flooding, for which the reservoir simulator already exists.

5. Utilizing the polymer flooding option of black-oil simulator

Following Zeinijahromi et al. (2013), let us introduce small (vanishing) adsorption $c_a(\gamma)$ via the amount of strained fine particles

$$c_a(\gamma) = \sigma_{a0} - \sigma_{cr}(\gamma) \tag{30}$$

into the salt mass balance Eq. (29):

$$\frac{\partial(\gamma s + \delta c_a(\gamma))}{\partial t} + \vec{\nabla}(\gamma f \vec{U}) = 0 \tag{31}$$

Here, δ is a small parameter. Defining the residual resistance factor RRF as

$$RRF = 1 + \beta\phi c^0 \delta\sigma_{a0} \tag{32}$$

transforms Eq. (27) to the form

$$\vec{U} = -k\left[\frac{k_{rw}(s)}{\mu_w(1+(RRF-1)\sigma_{a0}-\sigma_{cr}(\gamma)/\delta\sigma_{a0})} + \frac{k_{rg}(s)}{\mu_g}\right]\vec{\nabla} p \tag{33}$$

The fractional flow function in conservation laws (19) and (20) depends on saturation and salt concentration.

The assumptions of the discussed polymer flooding model and basic equations can be found in Schlumberger Information Solutions (SIS) (2008).

Finally, the system of equations for 2-phase flow with varying water salinity and fines mobilization (24), (26), (27), (29) can be "translated" into the polymer flooding model (24), (26), (31), (33) with the "dictionary" given by formulae (30) and (32). More detailed explanations can be found in Zeinijahromi et al. (2013). The mapping of the flow system "water with fines – gas" into that "water with polymer – compressible fluid" allows formulating the problem of fresh water bank injection in terms of the polymer flooding model, which will be solved numerically in the next section.

6. Results of reservoir simulation

A comparative study of the normal pressure depletion and that accompanied by fresh water bank injection into an abandoned down-dip well was performed using the black-oil model Eclipse 100 (Schlumberger Information Solutions (SIS), 2008). Two scenarios correspond to the left and right hand sides of Fig. 3

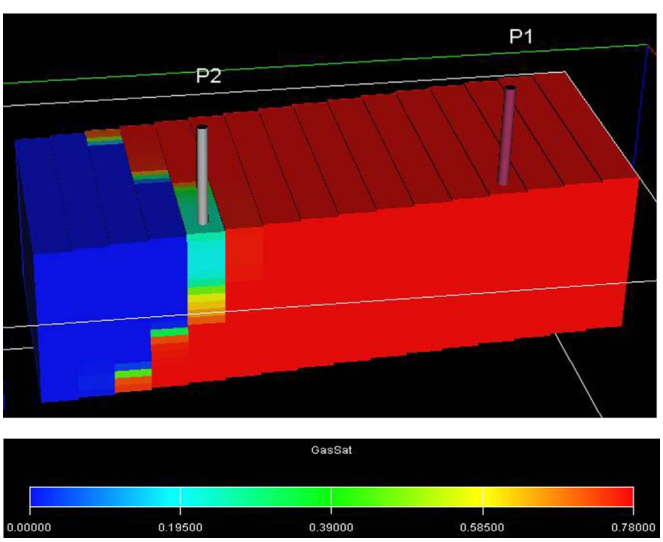

Fig. 5. Areal gas saturation distribution at the moment of abandonment of watered-up downdip well; gas saturation varies from zero (blue) to 0.78 (red). (For interpretation of the references to color in this figure legend, the reader is referred to the web version of this article.)

correspondingly. All reservoir and fluid properties, except permeability alteration in cells where the injected water invaded, were kept constant for both cases. The maximum retained concentration function over the reservoir was calculated using the model for $\sigma=\sigma_{cr}(\varepsilon)$ matched to the example data from Lever and Dawe (1984), see Fig. 4. Hence, it was assumed that the reservoir rock and fines had the same fines capture capacity as that used in the laboratory tests, i.e. fines primarily composed of clay, with the same mineral composition of rock and the same water salinity and pH.

The reservoir has a rectangular shape with an inclined angle of 25°. The gas is produced via two production wells P1 and P2 (Fig. 5). The initial water–gas contact is located 160 m from the down-dip well P2; the inter-well distance is 350 m. The layer cake reservoir was composed of 10 different permeability layers with the permeability decreasing with depth. The depth permeability variation is presented in Table 1. Three cases of low, medium and high heterogeneity, corresponding to variance coefficients of C_v=0.52, 0.72 and 0.92, respectively, have been considered (second, third and fourth lines in Table 1). These values represented essentially the homogeneous, mildly heterogeneous and very heterogeneous reservoirs, correspondingly (Jensen et al., 1997). The formation and aquifer waters were assumed to have 3% concentration of NaCl. Other reservoir and fluid properties are presented in Table 2.

Gas and water flow towards the producers before the abandonment of the down-dip well has been modeled using black-oil model for low compressible water and compressible gas. Fig. 5 shows the gas saturation field at the abandonment moment that corresponds to 0.30 water cut in well P2 for the case of highly heterogeneous reservoir. The invaded water front already passed the well in highly permeable layers with significantly less displacement in low permeable zones.

The reduction in field permeability after fresh water bank injection is presented in Fig. 6, which shows the side and top views on the altered permeability field after the injection of fresh water bank. The color scale corresponds to the permeability reduction ratio of $k(\sigma)/k_0$ with "red" indicating the maximum permeability reduction by14 times. The "blue" region correspond to areas where fresh water has not reached during the injection, i.e. $k(\sigma)/k_0$=1. Permeability increases from the injection point to the inner of the reservoir. During the injection, fresh water bank enters mostly the upper high permeability layers, causing maximum permeability reduction while the permeability reduction in low layers is significantly less. The short-term fresh water injection creates a barrier against the encroached water in the most permeable path. This leads to a significant delay in water finger encroachment towards up-dip well P1 as well as aids in the diversion of the invaded water to sweep the low permeable layers.

The first significant difference between the normal pressure blow down and that with the induced fines migration is evident from Fig. 7, where saturation fields are presented at the moment before water breakthrough at up-dip well for both field development scenarios. The vertical cross-sections in Fig. 8a and b show that the residual gas in low permeable layers is less for the case of fresh water injection. The residual gas near to producer P1 is also less for the fresh water injection case. Fig. 8 shows the top view of

Table 1
Horizontal permeability distribution in 10-layer-cake reservoir (mD).

	k_1	k_2	k_3	k_4	k_5	k_6	k_7	k_8	k_9	k_{10}
Low heterogeneity (C_v=0.29)	150	140	130	120	110	100	90	80	70	60
Medium heterogeneity (C_v=0.53)	210	160	140	120	110	100	80	60	50	20
High heterogeneity (C_v=0.72)	230	190	150	135	120	100	70	43	10	2

Table 2
Parameters used for the simulation model.

Parameters of the simulation model	Values
Node number (x, y, z)	$50 \times 50 \times 20$
The length of the reservoir (m)	660
The width of the reservoir (m)	300
The thickness of the reservoir (m)	15
Aquifer length (m)	1000
The length of perforated intervals (m)	9
Vertical permeability (mD)	5
Initial reservoir pressure (Psi)	4000
Viscosity of water (cP)	1
Viscosity of gas (cP)	0.017
Gas compressibility factor	1.107
Gas density (kg/m^3)	0.8
Initial water saturation	0.22
Porosity	0.2

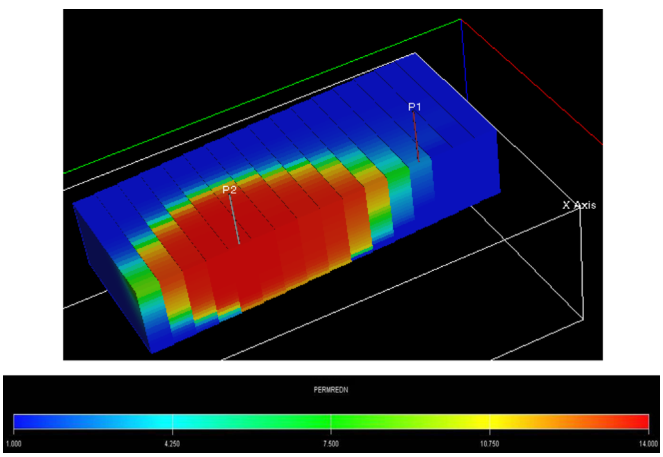

Fig. 6. Field permeability alteration after fresh water bank injection: creation of low permeable barrier: permeability decline ratio increases from 1.0 (blue) to 14 (red). (For interpretation of the references to color in this figure legend, the reader is referred to the web version of this article.)

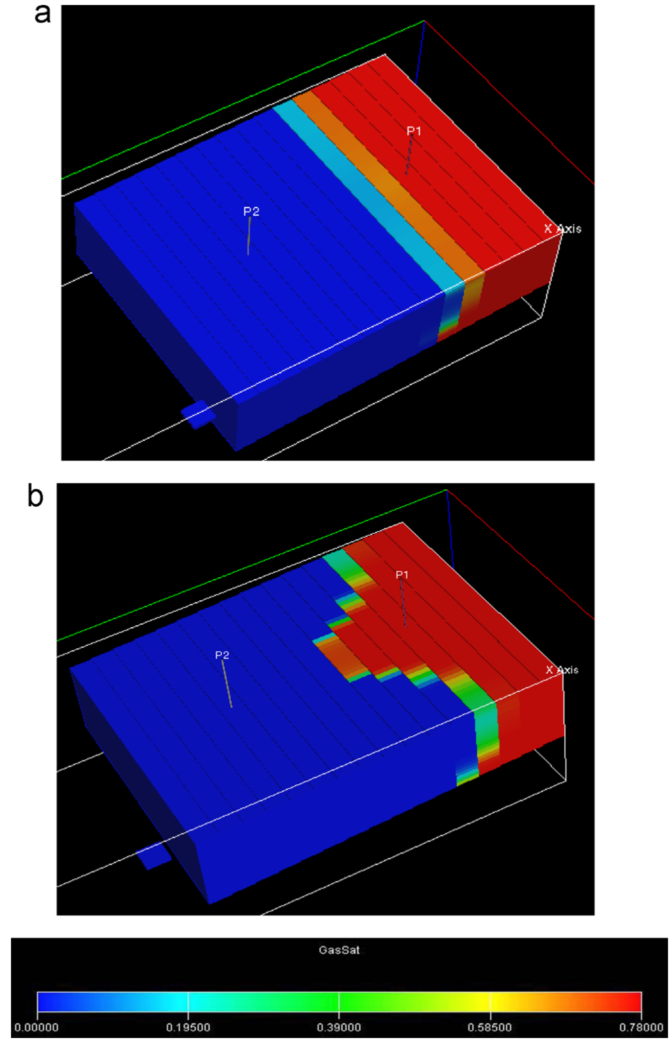

Fig. 7. Aquifer water encroaching and gas saturation distribution over the reservoir before water breakthrough at up-dip well P1: (a) normal pressure depletion and (b) the case of fresh water bank injection.

five low permeability layers, i.e. of the lower part of the reservoir, at the moment when water cut in up-dip well reaches the value f=0.30. The area of the maximum gas saturation, which corresponds to water saturation s=0.22, is higher for the normal depletion. Water saturation near to producer is also higher for the normal depletion scenario. Comparison between the images in Fig. 8a and b shows that the gas saturation decrease due to fresh water injection is more pronounced in the low permeability layers.

The effect of fresh water bank injection and the consequent permeability reduction around the abandoned well on gas recovery and water cut is shown in Fig. 9 for reservoirs with different heterogeneities (Table 3). The recovery dynamics before the down-dip well P2 abandonment is the same for the normal and fines-assisted depletion schemas (Fig. 9a). Points 1, 3 and 5 correspond to the well P2 abandonment in three different heterogeneity cases. Water cut in down-dip well P2 is also the same for three cases as shown by the continuous and dashed curves in Fig. 9b. As illustrated in Fig. 9a, the gas recovery is slightly lower for the case of fresh water injection until the moment of the well P1 abandonment for normal depletion (points 2, 4 and 6). This is due to the permeability reduction which causes some minor decrease of production rate and of water cut. These two competitive effects almost compensate each other resulting in approximately the same gas production. The bulk incremental gas recovery is achieved due to prolonged life of the up-dip well – gas production continues after moments 2, 4 and 6 in the reservoirs with different heterogeneity. As the low permeable zone acts as a barrier to the invading water flow, the velocity of the invaded water finger is slowed down considerably and is diverted to sweep the low permeable zones. The final recovery factor increases from 49% to 66% for low heterogeneity reservoir, from 52% to 68% for medium heterogeneity reservoir and from 55% to 70% for highly heterogeneous reservoir. Dashed water cut curves for the up-dip well P1 are significantly shifted to the right in the case of fresh water injection comparing to the continuous curves for normal depletion. It corresponds to the delayed watering of the up-dip well in the case of fines migration assisted gas production.

Fig. 10 shows the cumulative amount of invaded water for the normal and fines assisted pressure depletion in three cases of the reservoirs with different heterogeneity. The higher is the heterogeneity the faster is the water breakthrough to production wells and the higher is the amount of water invaded in the reservoir. Therefore, the continuous black, red and green curves are located in the decreasing order. The dashed curves are located significantly below the corresponding continuous curves, showing that the fresh water bank injection into abandoned wells results in the sizable decreasing of the invasion water volume. Induced fines migration improves water production mostly in highly heterogeneous reservoir, since it plugs preferentially the highly permeable layers (Fig. 6). The accumulated volume of invaded water

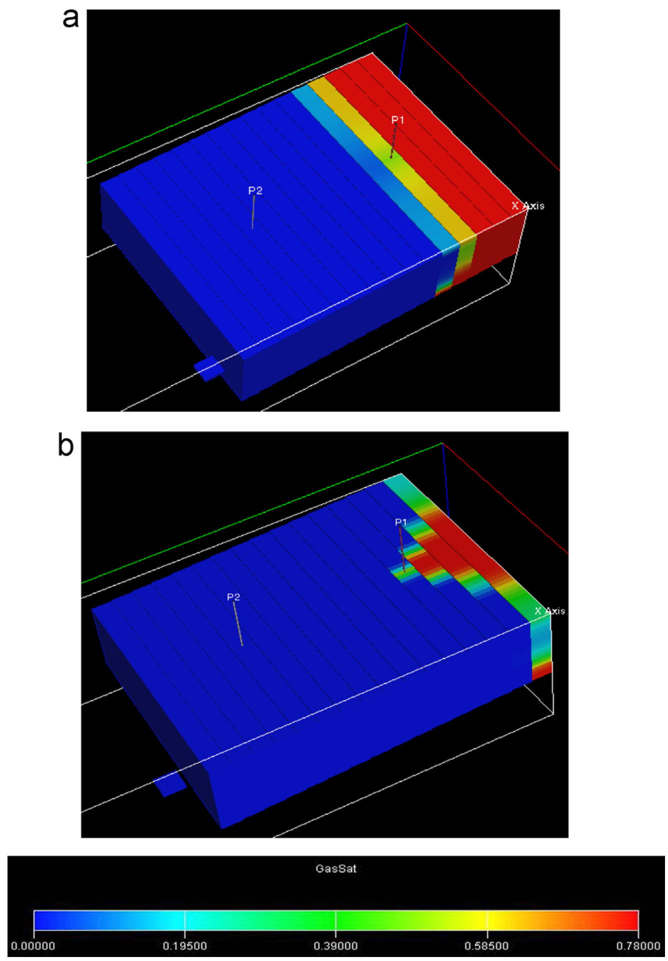

Fig. 8. Effects of fresh water bank injection on the sweep efficiency and residual gas at the moment of the field abandonment: (a) normal pressure depletion and (b) the case of fresh water bank injection.

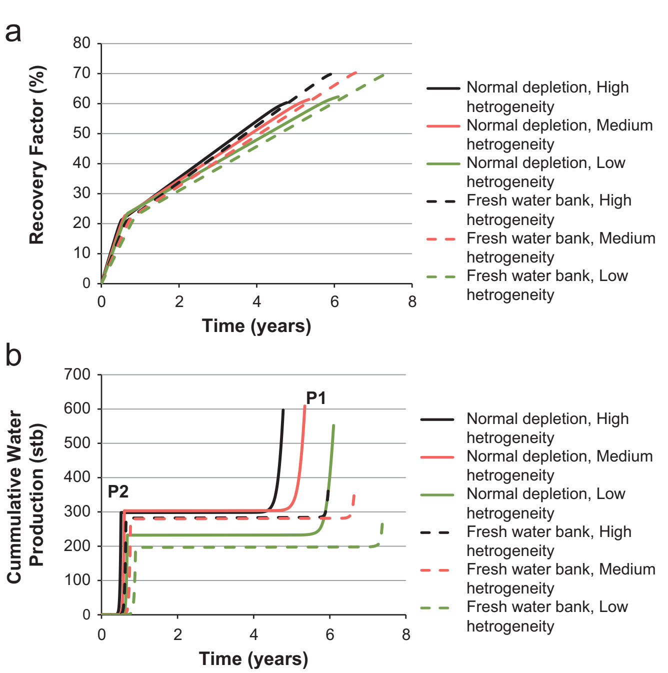

Fig. 9. Gas recovery versus time for “normal” and “fines-assisted” depletion: effects of heterogeneity: (a) recovery factor curve and (b) water cut.

Table 3
Effects of heterogeneity on incremental gas recovery.

Production method	Heterogeneity	Gas recovery factor	Abandonment time (years)
Normal pressure depletion	High	60	4.7
Pressure depletion with fresh water bank injection	Medium	61	5.3
Normal pressure depletion	Low	62	6
Pressure depletion with fresh water bank injection	High	70	5.9
Normal pressure depletion	Medium	70	7.4
Pressure depletion with fresh water bank injection	Low	70	6.6

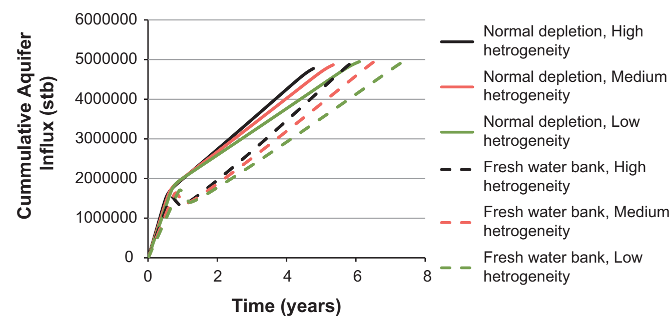

Fig. 10. Effect of fresh water bank injection on water influx. (For interpretation of the references to color in this figure, the reader is referred to the web version of this article.)

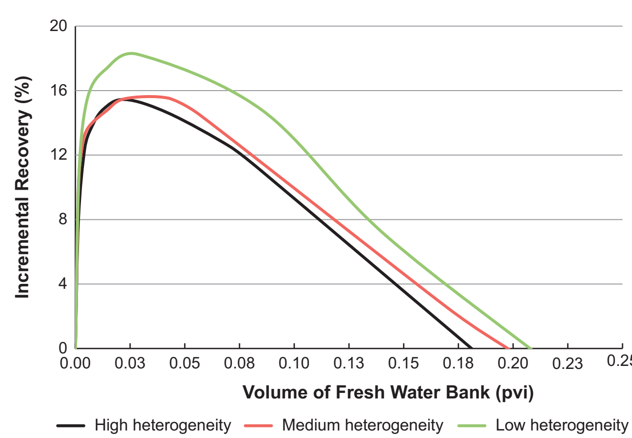

Fig. 11. Effect of fresh water bank volume on incremental gas recovery: existence of an optimal volume.

slightly decreases after fresh water bank injection, since some encroached water was pushed back to the aquifer during the injection; then it “recovers” and increases almost proportionally to time. So, the injection of fresh water bank into the abandoned watered-up well results in significant reduction of the aquifer water invaded into the reservoir.

Sensitivity study with respect to the fresh water volume injected is presented in Fig. 11. Different simulations have been performed for different bank sizes for normal and fines-assisted depletion (Krujisdjik et al., 2012). The incremental gas recovery monotonically increases from zero as the bank volume increases (left branches of the curves). However, excessively high injected volumes would contribute to the well watering; thus an increase in already high bank volume leads to the decrease of incremental recovery (right branches). Hence, there does exists an optimal size of the injected fresh water volume, which is not too small to allow the invading water passing through whilst sufficient to create a significant flow barrier against the invading water. The optimal volume is not too large to contribute to the water production. The optimal slug size for low heterogeneity, medium heterogeneity and high heterogeneity is 0.028, 0.016 and 0.022 PV, respectively. These correspond to the injection time of 18 days, 10 days and 14 days, correspondingly.

7. Summary and discussions

Injection of a small volume fresh water bank into abandoned watered-up downdip wells forms a low permeable barrier against the invaded aquifer water. The formation damage induced by migrating fines is localized near to abandoned producer, i.e. far away from the producing wells; it almost does not affect their productivity index. The mobilized fines strain the water-filled pores; it decreases the phase permeability for water and almost does not affect gas phase permeability. Therefore, the main physics effects of the improved gas recovery are slowing down the invading water and the prolongation of the exploitation period of the up dip wells due to released fines and the consequent permeability reduction. It results in decreased residual gas after the overall well abandonment and, finally, in an increased gas recovery.

The system of governing equations consists of seven equations for mass balance of water, gas, fine particles and salt, of maximum retention function, of kinetics for particle straining and of generalized Darcy's law for two-phase flow under the particle retention. The unknowns in the system are water saturation, pressure, concentration of suspended, attached and strained particles, salt concentration and flow velocity. The system can be solved numerically, which would require the development of the corresponding reservoir simulator. Possibly, this is still required for matching the core flood data on simultaneous commingled core flood by gas and low salinity water. Yet, in large scale approximation, where the free run length of lifted fines is significantly smaller than the inter well distance, the system can be significantly simplified due to instant size exclusion of the mobilized fines; the number of equations is reduced to five. Due to such simplification, the polymer flooding black-oil model can be used to simulate the fines migration assisted improved gas recovery.

Nevertheless, several restrictive assumptions have been made in order to model the process by a conventional numerical simulator. First, the maximum retention function is independent of saturation, i.e. the gradual particle release during continuous water saturation increase in each reservoir point is not captured by the model. So, the model exhibits the fines release from the overall matrix surface due to salinity decrease only. Yet, the salt concentration front delays comparing to the saturation front; thus, at the moment of the salt concentration front arrival to the reservoir point, water saturation there is already high. A thorough literature search revealed that the release and capture of fine particles in a porous medium has only been investigated in the presence of single phase water (Lever and Dawe, 1984; Valdya and Fogler, 1992; Khilar and Fogler, 1998; Civan, 2010). The effect of residual gas saturation on fines mobilization must be investigated both experimentally and theoretically.

Another assumption is the fixed permeability value after the fresh water injection stops. In reality, the injected fresh water is transported by the invading saline water towards the updip well, resulting in further decrease in water velocity. Yet, since the fresh water volume is small if compared to the pore volume of the overall reservoir, the dissolution of the bank in the saline water drive will occur long before it would reach the updip well, adjusting the above assumption. Neglecting the effect of further permeability decrease after the injection stops underestimates the incremental gas recovery.

The above limitations of the model mean that the results of this analysis are indicative only. More realistic estimates of the reservoir behavior and the efficiency of the induced fines migration due to creation of the low permeable barrier against the encroaching water require the implementation of the saturation-dependent maximum retention function into a numerical reservoir simulator.

The effects of pH and temperature difference between the injected and formation waters can be modeled in a similar way as the effects of the salinity difference. In the case of pH difference, the mass balance equation for base component substitutes the mass balance equation for salt. For hot water injection, the energy balance is included into the governing system of equations instead of the mass balance equation for salt.

Injection of fresh water bank for slowing down the encroaching water is effective for the reservoirs containing retained fines. Usually, it is the case in low consolidated rocks containing some loose non-clay material like silts, quartz, mica and silica particles. High clay contents sandstones are also promising candidates for the proposed method (Bennion et al., 1996, 2000; Bennion and Thomas, 2005; Byrne and Waggoner, 2009). The kaolinite and illite clays are reported to release fines due to decrease of salinity, pH increase or increase of the temperature (Khilar and Fogler, 1998).

The mathematical model (15)–(18) also describes the natural effect of different reservoir and aquifer water compositions on gas recovery during pressure depletion with strong water support. The difference in water compositions is due to subterranean water movement with solute transport after the gas accumulation has already been formed. If the aquifer water has lower salinity or higher pH than the formation water, the invasion of water into the reservoir during the depletion rises fines, decreases the permeability in swept zones and slows down the encroached water. It results in decreased water cut, prolonged life of production wells before abandonment and incremental gas recovery. These effects are more likely happen in fields with high clay contents or in low consolidated rocks with free silts. Application of the model (15)–(18) would allow accounting for the above mentioned effects on optimal well placing, depletion rates and gas recovery during conventional gas depletion.

8. Conclusions

Mathematical modeling of two–phase immiscible flow with fines migration and the development of the fines migration assisted method for enhanced gas recovery allow the following conclusions: (1) System of two-phase immiscible compressible flow with maximum particle retention function describes injection of fresh water bank into watered-up abandoned gas wells with high water cut during the pressure depletion of gas fields with strong water support. (2) Injection of a small fresh water volume into abandoned gas well results in fines mobilization, capture and permeability decline in the invaded water paths. Those phenomena cause the decrease in water cut, prolonged life of the up-dip producer wells and, finally, an increase of the reservoir gas recovery. (3) Increasing the small volume of the injected fresh water results in the increased zone of permeability reduction against the aquifer water invasion. Increasing the large volume of injected fresh water results in the increased water cut and decreased incremental recovery. Therefore, for a given reservoir, there does exist an optimal fresh water bank size. (4) For the investigated reservoirs, the optimal bank size is 1.5–3% of the reservoir pore volume with the injection duration of 1.5–3 weeks. The incremental gas recovery is 15–18%. (5) System of two-phase immiscible compressible flow with maximum particle retention function describes also the case of the pressure depletion in gas fields with strong water support, where the reservoir fines are mobilized by the invaded aquifer water due to the difference in aquifer and formation water compositions.

Acknowledgments

Authors are in a great debt to Prof. Ashok Khurana for clear explanation of the water blocking problems. Many thanks are due to T. Rodrigues, I. Abbasy, K. Boyle (Santos Ltd., Australia) and F. Machado, A.L.S. de Souza (Petrobras, Brazil) for detailed discussions of the field applications, for support and encouragement. PB is grateful to Prof. P. Currie (Delft University of Technology) and Prof. A. Shapiro (Technical University of Denmark) for long-time co-operation in formation damage. Dr. A. Badalyan and Dr. T. Carageorgos (The University of Adelaide) are gratefully acknowledged for improving the quality of the text. The work is sponsored by Santos Ltd. and by two grants of Australian Research Council (ARC).

References

Bedrikovetsky, P., 2008. Upscaling of stochastic micro model for suspension transport in porous media. Transp. Porous Media 75 (3), 335–369.
Bedrikovetsky, P., et al., 2011. Modified particle detachment model for colloidal transport in porous media. Transp. Porous Media 86 (2), 353–383.
Bennion, D.B., Thomas, F.B., Bietz, R.F., 1996. Low permeability gas reservoirs: problems, opportunities and solutions for drilling, completion, stimulation and production. In: Proceedings of the SPE Gas Technology Symposium, 28 April–1 May. SPE Paper 35577. Calgary, Alberta, Canada.
Bennion, D.B., Thomas, F.B., Ma, T., 2000. Formation damage processes reducing productivity of low permeability gas reservoirs. In: Proceedings of the SPE Rocky Mountain Regional/Low-Permeability Reservoirs Symposium and Exhibition, 12–15 March. SPE Paper 60325. Denver, Colorado, USA.
Bennion, D.B., Thomas, F.B., 2005. Formation damage issues impacting the productivity of low permeability, low initial water saturation gas producing formations. J. Energy Resour. Technol. 127 (3), 240–247.
Bergendahl, J., Grasso, D., 2000. Prediction of colloid detachment in a model porous media: hydrodynamics. J. Chem. Eng. Sci. 55 (9), 1523–1532.
Bradford, S., Torkzaban, S., 2008. Colloid transport and retention in unsaturated porous media: a review of interface-, collector-, and pore-scale processes and models. Vadose Zone J. 7 (2), 667–681.
Bradford, S., et al., 2009. Coupled factors influencing concentration-dependent colloid transport and retention in saturated porous media. J. Environ. Sci. Technol. 43 (18), 6996–7002.
Braedley, H.B., 1987. Petroleum Engineering Handbook. Society of Petroleum Engineers.
Byrne, M.T., Waggoner, S.M., 2009. Fines migration in a high temperature gas reservoir—laboratory simulation and implications for completion design. In: Proceedings of the 8th European Formation Damage Conference, 27–29 May. SPE Paper 121897. Scheveningen, The Netherlands.
Byrne, M.T., Slayter, A.G., McCurdy, P., 2010. Improved selection criteria for sand control: when are "fines" fines? In: Proceedings of the SPE International Symposium and Exhibiton on Formation Damage Control, 10–12 February. SPE Paper 128038. Lafayette, Louisiana, USA.
Chauveteau, G., Nabzar, L., Coste, J., 1998. Physics and modeling of permeability damage induced by particle deposition. In: Proceedings of the SPE Formation Damage Control Conference, 18–19 February. SPE Paper 39463. Lafayette, Louisiana, USA.
Cinar, Y., et al., 2006. An experimental and numerical investigation of crossflow effects in two-phase displacements. SPE J. 11 (2), 216–226.
Cinar, Y., Marquez, S., Orr, F.J., 2007. Effect of IFT variation and wettability on relative permeability. SPE Reserv. Eng. Eval. 10 (3), 211–220.
Civan, F., 2007. Reservoir Formation Damage: Fundamentals, Modeling, Assessment, and Mitigation. Gulf Professional Publishing, Elsevier, Burlington p. 1114.
Civan, F., 2010. Non-isothermal permeability impairment by fines migration and deposition in porous media including dispersive transport. J. Transp. Porous Media 85 (1), 233–258.
Cortis, A., et al., 2006. Transport of cryptosporidium parvum in porous media: long-term elution experiments and continuous time random walk filtration modeling. J. Water Resour. Res. 42, 12.
Derjaguin, B., 1989. Theory of Stability of Colloids and Thin Films. Springer Verlag, Dordrecht.
Fogden, A., et al., 2011. Mobilization of fine particles during flooding of sandstones and possible relations to enhanced oil recovery. Energy Fuels 25 (4), 1605–1616.
Freitas, A., Sharma, M., 2001. Detachment of particles from surfaces: an Afm study. J. Colloid Interface Sci. 233 (1), 73–82.
Gitis, V., et al., 2010. Deep-bed filtration model with multistage deposition kinetics. Chem. Eng. J. 163 (1–2), 78–85.
Gravelle, A., et al., 2011. Experimental Investigation and modelling of colloidal release in porous media. Transp. Porous Media 88 (3), 441–459.
Israelachvili, J.N., 1992. Intermolecular and Surface Forces. Academic press, London.
Jensen, J., et al., 1997. Statistics for Petroleum Engineers and Geoscientists. Prentice Hall PTR, New Jersey p. 1997.
Jiao, D., Sharma, M.M., 1994. Mechanism of cake buildup in crossflow filtration of colloidal suspensions. J. Colloid Interface Sci. 162 (2), 454–462.
Ju, B., et al., 2007. A new simulation framework for predicting the onset and effects of fines mobilization. Transp. Porous Media 68 (2), 265–283.
Karp, J.C., Lowe, D.K., Marusov, N., 1962. Horizontal barriers for controlling water coning. SPE J. Pet. Technol. 14 (7), 783–790.
Khilar, K., Fogler, H., 1998. Migrations of Fines in Porous Media. Kluwer Academic Publishers, Dordrecht/London/Boston.
Krujisdjik, van C, Farajzadeh, R., Mahani, H., Glasbergen, G., 2011, 2012. Personal communications.
Kumar, M., et al., 2010. Mechanisms of improved oil recovery from sandstone by low salinity flooding. In: Proceedings of the International Symposium of the Society of Core Analysts, 4–7 October. Paper SCA2010-25. Halifax, Nova Scotia, Canada.
Lever, A., Dawe, R., 1984. Water-sensitivity and migration of fines in the Hopeman sandstone. J. Pet. Geol. 7 (1), 97–107.
Lin, H.-K., et al., 2009. Attachment and detachment rate distributions in deep-bed filtration. Phys. Rev. E 79 (4), 046321-1–046321-12.
Mahani, H., et al., 2011. Analysis of field responses to low-salinity waterflooding in secondary and tertiary mode in Syria. In: Proceedings of the SPE EUROPEC/EAGE Annual Conference and Exhibition, 23–26 May. SPE Paper 142960. Vienna, Austria.
Massoudieh, A., Ginn, T.R., 2010. Colloid-facilitated contaminant transport in unsaturated porous media. In: Hanrahan, G. (Ed.), Modelling of Pollutants in Complex Environmental Systems. ILM Publications, Hertfordshire, Glensdale, p. 263.
Miranda, R.M., Underdown, D.R., 1993. Laboratory measurement of critical rate: a novel approach for quantifying fines migration problems. In: Proceedings of the SPE Production Operations Symposium, 21–23 March. SPE 25432. Oklahoma City, Oklahoma, USA.
Mojarad, R., Settari, A., 2007. Coupled numerical modelling of reservoir flow with formation plugging. J. Can. Pet. Technol. 46 (3), 54–59.
Muecke, T.W., 1979. Formation fines and factors controlling their movement in porous media. J. Pet. Technol. 31 (2), 144–150.
Nabzar, L., Chauveteau, G., Roque, C., 1996. A new model for formation damage by particle retention. In: Proceedings of the SPE Formation Damage Control Symposium, 14–15 February. SPE Paper 1283. Lafayette, Louisiana, USA.
Ochi, J., Vernoux, J.-F., 1998. Permeability decrease in sandstone reservoirs by fluid injection: hydrodynamic and chemical effects. J. Hydrol. 208 (3), 237–248.
Pang, S., Sharma, M.M., 1997. A model for predicting injectivity decline in water-injection wells. SPE Form. Eval. 12 (3), 194–201.
Payatakes, A., Tien, C., Turian, R.M., 1973. A new model for granular porous media: part I. Model formulation. AIChE J. 19 (1), 58–67.
Payatakes, A., Rajagopalan, R., Tien, C., 1974. Application of porous media models to the study of deep bed filtration. Can. J. Chem. Eng. 52 (6), 722–731.
Rousseau, D., Latifa, H., Nabzar, L., 2008. Injectivity decline from produced-water reinjection: new insights on in-depth particle-deposition mechanisms. SPE Prod. Oper. 23 (4), 525–531.
Sarkar, A., Sharma, M., 1990. Fines migration in two-phase flow. J. Pet. Technol. 42 (5), 646–652.
Schechter, R.S., 1992. Oil Well Stimulation. Society of Petroleum Engineers, Richardson, TX.
Schembre, J.M., Kovscek, A.R., 2004. Thermally induced fines mobilization: its relationship to wettability and formation damage. In: Proceedings of the SPE International Thermal Operations and Heavy Oil Symposium and Western Regional Meeting, 16–18 March. SPE Paper 86937. Bakersfield, California, USA.
Schlumberger Information Solutions (SIS), 2008. Eclipse Reservoir Engineering Software. Schlumberger Limited. Available online.
Shapiro, A.A., 2007. Elliptic equation for random walks, application to transport in microporous media. Phys. A: Stat. Mech. Appl. 375 (1), 81–96.
Sharma, M.M., Yortsos, Y.C., 1987. Fines migration in porous media. AIChE J. 33 (10), 1654–1662.
Takahashi, S., Kovscek, A.R., 2010. Wettability estimation of low-permeability, siliceous shale using surface forces. J. Pet. Sci. Eng. 75 (1–2), 33–43.
Tiab, D., Donaldson, E.C., 2004. Petrophysics: Theory and Practice of Measuring Reservoir Rock and Fluid Transport Properties. Gulf Professional Publication, MA, USA.
Tufenkji, N., 2007. Colloid and microbe migration in granular environments: a discussion of modelling methods. In: Frimmel, F.H., von der Kammer, F., Flemming, F.-C. (Eds.), Colloidal Transport in Porous Media. Springer-Verlag, Berlin, pp. 119–142.
Valdya, R., Fogler, H., 1992. Fines migration and formation damage: influence of pH and ion exchange. SPE Prod. Eng. 7 (4), 325–330.
Van Oort, E., Van Velsen, J.F.G., Leerlooijer, K., 1993. Impairment by suspended solids invasion: testing and prediction. SPE Prod. Facil. 8 (3), 178–184.

Yuan, H., Shapiro, A., 2010a. Modeling non-fickian transport and hyperexponential deposition for deep bed filtration. Chem. Eng. J. 162 (3), 974–988.
Yuan, H., Shapiro, A., 2010b. A mathematical model for non-monotonic deposition profiles in deep bed filtration systems. Chem. Eng. J. 166 (1), 105–115.
Zaitoun, A., Pichery, T., 2001. A successful polymer treatment for water coning abatement in gas storage reservoir. In: Proceedings of the SPE Annual Technical Conference and Exhibition, 1–3 January. SPE Paper 71525. New Orleans, Louisiana, USA.
Zeinijahromi, A., Lemon, P., Bedrikovetsky, P., 2011. Effects of Induced migration of fines on water cut during waterflooding. J. Pet. Sci. Eng. 78, 609–617.
Zeinijahromi, A., Vaz, A., Bedrikovetsky, P.G., Borazjani, S., 2012. Effects of Fines migration on well productivity during steady state production. J. Porous Media 15 (7), 665–679.
Zeinijahromi, A., Nguyen, T.K.P., Bedrikovetsky, P., 2013. Mathematical model for fines migration assisted waterflooding with induced formation damage. J. Soc. Pet. Eng. SPEJ 18 (3), 447–457.